




## Article

# Biodiesel Production from Waste Frying Oil (WFO) Using a Biomass Ash-Based Catalyst

Benjamín Nahuelcura <sup>1,2</sup>, María Eugenia González <sup>3,4,\*</sup> , Nicolas Gutierrez <sup>1</sup> , Jaime Nanculeo <sup>5</sup>  
and Juan Miguel Romero-García <sup>6</sup> 

<sup>1</sup> Department of Mechanical Engineering, University of La Frontera, Temuco 4780000, Chile; b.nahuelcura01@ufromail.cl (B.N.); nicolas.gutierrez@ufrontera.cl (N.G.)

<sup>2</sup> Master Program in Engineering Sciences, Faculty of Engineering and Sciences, University of La Frontera, Temuco 4780000, Chile

<sup>3</sup> Department of Chemical Engineering, University of La Frontera, Temuco 4780000, Chile

<sup>4</sup> Scientific and Technological Bioresources Nucleus-BIOREN, University of La Frontera, Temuco 4780000, Chile

<sup>5</sup> Doctoral Program in Engineering Sciences with Specialization in Bioprocesses, Faculty of Engineering and Sciences, University of La Frontera, Temuco 4780000, Chile; jaime.nanculeo@ufrontera.cl

<sup>6</sup> Department of Chemical, Environmental and Materials Engineering, Centre for Advanced Studies in Earth Sciences, Energy and Environment (CEACTEMA), Universidad de Jaén, 23001 Jaén, Spain; jrgarcia@ujaen.es

\* Correspondence: mariaeugenia.gonzalez@ufrontera.cl

**Abstract:** Biodiesel, an eco-friendly alternative to conventional fossil fuels, offers reduced emissions like carbon dioxide, sulfur oxides, and soot. This study explores biodiesel production from a blend of waste oils using a novel biomass-based catalyst derived from the bottom ash of a biomass boiler. Catalyst synthesis involved wet impregnation, a unique approach using previously unreported bottom ash. Characterization via SEM-EDS, BET, FTIR, and XRD revealed its composition and structure. Optimization of biodiesel production involved assessing alcohol molar ratio, catalyst concentration, and reaction time, achieving a maximum FAME concentration of 95% under specific conditions. Blending residual palm oil with waste frying oil enhanced biodiesel properties, demonstrating a maximum FAME concentration at specific catalyst concentration (8%), molar ratio (1:10), and reaction time (2 h). Catalyst reusability, up to three cycles without significant yield variation, showcased its sustainability. The catalyst, primarily composed of calcium, a characteristic biomass bottom ash component, exhibited mesoporous features. Impregnation with eggshells not only altered composition but also ensured a uniform particle size distribution. FTIR and XRD analyses indicated calcium in hydroxide and crystallized forms. Effective catalyst separation methods included decanting or water washing, with optimal biodiesel purity achieved through 3% phosphoric acid washing at 60 °C. Various recovery methods were assessed, highlighting hexane washing as the most efficient, enabling up to three catalyst reuse cycles without substantial efficiency loss.

**Keywords:** biodiesel; bottom ash; catalyst; waste; biomass



**Citation:** Nahuelcura, B.; González, M.E.; Gutierrez, N.; Nanculeo, J.; Romero-García, J.M. Biodiesel Production from Waste Frying Oil (WFO) Using a Biomass Ash-Based Catalyst. *Catalysts* **2024**, *14*, 553. <https://doi.org/10.3390/catal14080553>

Academic Editors: Vincenzo Vaiano and Olga Sacco

Received: 5 January 2024

Revised: 5 February 2024

Accepted: 8 February 2024

Published: 22 August 2024



**Copyright:** © 2024 by the authors. Licensee MDPI, Basel, Switzerland. This article is an open access article distributed under the terms and conditions of the Creative Commons Attribution (CC BY) license (<https://creativecommons.org/licenses/by/4.0/>).

## 1. Introduction

Biodiesel is a fuel made up of monoalkyl esters of long-chain fatty acids, obtained through the transesterification process, derived from vegetable oils or animal fats, hence the definition of Fatty Acids Methyl Ester (FAME) [1]. The carbon cycle of biodiesel from sustainable resources can be considered carbon neutral, because oil plants absorb more CO<sub>2</sub> than that produced in the combustion of biodiesel. Thus, its use can effectively reduce CO<sub>2</sub> emission, protect the environment, and maintain ecological balance, compared to the use of fossil fuels [2]. This is further reinforced by using used frying/cooking oils (WFO/WCO) as a source of raw material for the production of biodiesel [3], which can be two to three times cheaper than using virgin vegetable oils and also allows the reuse of oils that are no longer fit for human consumption [4].

Transesterification, the most common process to produce biodiesel, consists of an equilibrium reaction, which describes the alcoholysis of the carboxylic esters and is usually carried out in the presence of a catalyst (e.g., NaOH and KOH, when referring to basic catalysts) [5,6]. Homogeneous catalysts are the most widely used for large-scale biodiesel production; however, they are usually toxic, highly flammable, and corrosive by nature [7]. On the other hand, working with heterogeneous or solid catalysts provides similar performance to homogeneous catalysts but avoids these drawbacks; further, they do not dissolve in the reaction mixture, which facilitates their subsequent separation [8]. Solid basic catalysts are characterized by a high specific surface area and a high concentration of alkaline sites, which ensures high catalytic activity [9]. The most commonly used solid catalysts include metal oxides and transition metal oxides such as MgO, CaO, SrO, and BaO, among others [10]. These types of oxides, in particular calcium oxide, can be obtained from ashes resulting from combustion or calcination processes of wastes from the food, agriculture, and forestry industries. Research has been carried out with rice straw and husks [11,12], rice husks impregnated with eggshells [13], animal bones [14], and tree leaves [15], for example.

Bottom ash is part of the non-combustible material formed in thermal power plant burners. It is composed of the larger, heavier particles of ash that are deposited and which accumulate at the bottom of the boiler rather than being carried away by the flue gases [16]. The valorization of this waste is variable; in some countries, such as Germany, Japan, Denmark, and the Netherlands, bottom ash is widely used in roads, concrete, soil amendments, and soundproofing walls, achieving a reuse of around 90% [17]. In countries with less infrastructure, such as Canada, as of 2013, most of the ash (65%) was deposited in landfills [18].

The main components of bottom ash are calcium (Ca), potassium (K), magnesium (Mg), silicon (Si), and phosphorus (P), with the elemental composition varying according to the fuel used [19]. One of the main components of wood waste ash is calcium carbonate ( $\text{CaCO}_3$ ) [20]; calcining this compound at high temperatures reduces the presence of carbon and oxygen, increasing the concentration of species such as CaO allowing the use of the ash as a catalyst for biodiesel synthesis [7,21,22]. Further increasing the presence of CaO can be achieved by adding other organic wastes such as eggshells to the ash using the wet impregnation technique [12,13,23,24].

Based on the above, the utilization of bottom ash from a thermal power plant as heterogeneous base catalysts for biodiesel production was explored in this work. The final disposal of bottom ash in landfills generates a waste management problem due to the use of space and the loss of the opportunity to obtain interesting products from its valorization. That is why it is important to look for ways to use this waste.

## 2. Results

The following nomenclatures have been defined to designate the samples analyzed in this section: raw bottom ash (RBA) for the material collected directly from the boiler, calcined bottom ash (CBA) for the material treated in a muffle furnace at 900 °C, and calcium oxide impregnated ash (BAC) for the result obtained after the process described in this section.

### 2.1. Catalyst Characterization

BET analysis was not performed for the crude ash (RBA) because the degasification process prior to the analysis could eliminate certain components in the sample, making the results unrepresentative. The raw ash (RBA) presents a high level of calcium in its composition (Table 1), similar to that reported in ashes from other types of woody biomass. The EDS analysis does not show the presence of silicon; this is explained in that bottom ash usually concentrates particles of higher weight, while on the other hand, silicon is usually present in fly ash that is carried away by combustion gases [25,26].

The specific surface area for ash impregnated with calcium (BAC) is  $10.60 \text{ m}^2/\text{g}$ , close to values reported for other types of woody residue ash ( $8.98 \text{ m}^2/\text{g}$ ) [27], and similar to that reported for ash from other residues, such as rice husk ( $10.54 \text{ m}^2/\text{g}$ ) [12]. In general, samples with high calcium content and subjected to calcination processes above  $800^\circ\text{C}$  have similar surface area. The decrease in surface area is similar to what occurred in other cases where the same technique was used [12,24]. Such decrease is related to the deposition of calcium on the pores of the ash, which decreases its surface area but increases its capacity as a catalyst. Regarding the pore diameter, the biomass bottom ash studied qualifies as a mesoporous material (with pore diameter between 2 to 50 nm according to IUPAC classification). Finally, the particle size distribution (Figure 1) shows that the ash subjected to wet impregnation has a more uniform particle size, which could influence the availability of active sites to catalyze the transesterification reaction. It has been reported that the hydration/dehydration process in calcium oxide provides greater availability of active sites, since it breaks its crystals and allows a more homogeneous arrangement [28], which also generates a more uniform particle size.

**Table 1.** Elemental composition and textural properties of RBA, CBA, and BAC samples.

Sample	Composition								Specific Surface Area ( $\text{m}^2/\text{g}$ )	Pore Diameter (nm)	Pore Volume ( $\text{cc/g}$ )
	Ca	Mg	Na	K	Al	P	Si	C			
RBA	77.80	2.48	-	2.85	0.95	1.12	-	15.82	-	-	-
CBA	85.69	5.52	-	3.16	-	2.07	-	3.42	11.75	3.83	0.019
BAC	89.05	3.38	-	-	-	0.88	-	6.33	10.60	4.52	0.011

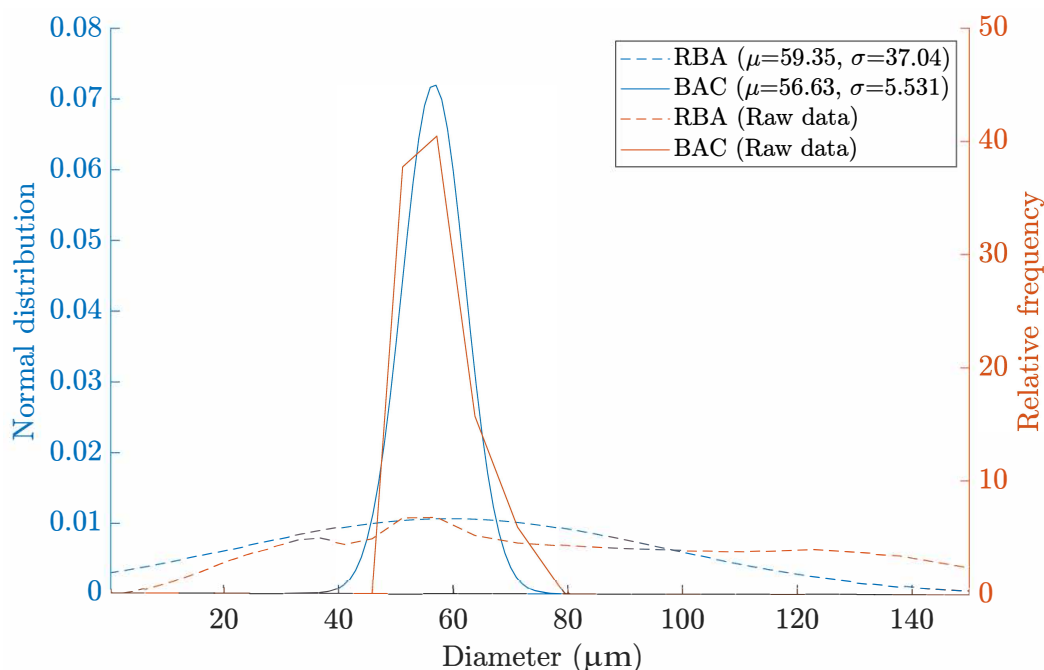


**Figure 1.** Particle size distribution fit for RBA and BAC samples. A noticeable difference in variance is observed, which indicates a more homogeneous particle size in the prepared catalyst.

The results of the FTIR (Figure 2) analysis show signal peaks for wavenumber  $3641 \text{ cm}^{-1}$ , associated with the vibration of O–H bonds, in particular those related to metallic elements such as calcium, in the form of hydroxide [29]. The wavenumber of  $1398 \text{ cm}^{-1}$  indicates the presence of carbonate ions ( $\text{CO}_3^{2-}$ ) [30], while the wavenumbers of  $872 \text{ cm}^{-1}$  and  $711 \text{ cm}^{-1}$  correspond to other forms of carbonate ion ordering ( $\nu_2 \text{ CO}_3^{2-}$  and  $\nu_4 \text{ CO}_3^{2-}$ , respectively) [31,32]. The wavenumber of  $1030 \text{ cm}^{-1}$  can be associated with the presence of

apatite [32], while  $604\text{ cm}^{-1}$  may indicate deposits of apatite in its crystallized form [32,33], or the presence of calcium sulfate [34], but the catalyst does not present sulfur in its composition so this option is discarded. It is concluded that calcination of RBA allowed the removal of residual carbon in the form of carbonate. This was sustained by the decrease in the intensity of all associated bands, the same assumption by which eggshell is calcined to produce CaO [35]. Furthermore, the differences for the  $3641\text{ cm}^{-1}$  band indicates that the metal species released by the decomposition of the carbonate ions migrated to their hydroxide form; this effect is even more noticeable for BAC, which is related to the wet impregnation of CaO, which was precisely to hydrate the oxide and thus facilitate its deposition on CBA.

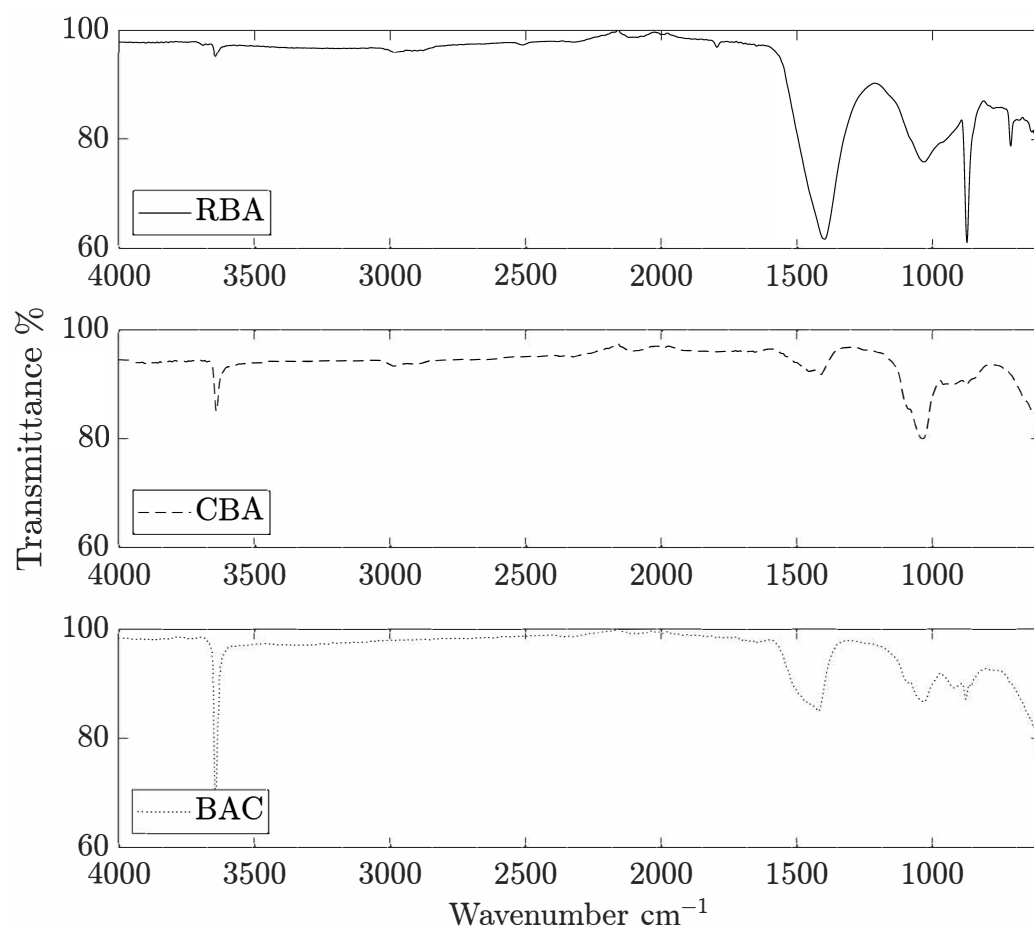


**Figure 2.** FTIR spectra for raw bottom ash RBA, calcined bottom ash CBA, and catalyst (ash/CaO BAC) samples.

An interesting result is that BAC presents a spectrum very similar to the mineral portlandite, one of the components of Portland cement [36], used as a binder in the concrete production.

Regarding the XRD analysis (Figure 3), in the raw ash (RBA) the spectrum is compatible with calcium carbonate ( $2\theta = 23.0^\circ, 29.4^\circ, 39.7^\circ$ , and  $43.4^\circ$ ), which confirms what was obtained both from the EDX and FTIR analysis. For calcinated bottom ash (CBA), peaks ( $2\theta = 32.2^\circ, 37.4^\circ$ ) corresponding to the calcium oxide (CaO) crystalline phase were observed after calcination of the bottom ash, indicating the transformation of  $\text{CaCO}_3$  into CaO [37]. For the peaks  $2\theta = 17.9^\circ, 31.5^\circ$ , and  $34.0^\circ$ , the spectrum matches calcium hydroxide  $\text{Ca(OH)}_2$  [38]. However, the peak at position  $2\theta = 34.06^\circ$  in addition to the peak at  $29.0^\circ$  may also indicate the presence of calcium phosphate or apatite [39,40]. Overall, the results with respect to the crystalline structures of the samples are in agreement with other work conducted with woody-type biomass ash, such as gasification ash [27], wood pellet

ash [37], and babul (*Acacia nilotica*) wood ash [41], with a predominant presence of  $\text{CaCO}_3$  in the raw material, which is transformed to  $\text{CaO}$  after calcination at  $800^\circ\text{C}$  [27]. However, the absence of elements such as silicon in the elemental composition generates differences with respect to other samples originating from similar processes, such as bottom ash from combustion boilers [25,26] or rice husk ash impregnated with  $\text{CaO}$  [12], where calcination or impregnation results in the formation of dicalcium silicate ( $\text{Ca}_2\text{SiO}_4$ ), a compound with higher stability with respect to catalyst reuse compared to other non-silicon compounds. The high percentage of calcium in the sample, with traces of phosphorus, added to the wet impregnation process, generated a catalyst composed mainly of calcium hydroxide and, to a lesser extent, hydrated calcium phosphate ( $\text{Ca}_5(\text{PO}_4)_3\text{OH}$ ) [39]. The use of ash together with calcium oxide avoids some of the complications that calcium oxide has when used alone, such as rapid deactivation in consecutive cycles, prolonged reaction time, or more severe reaction conditions [42].

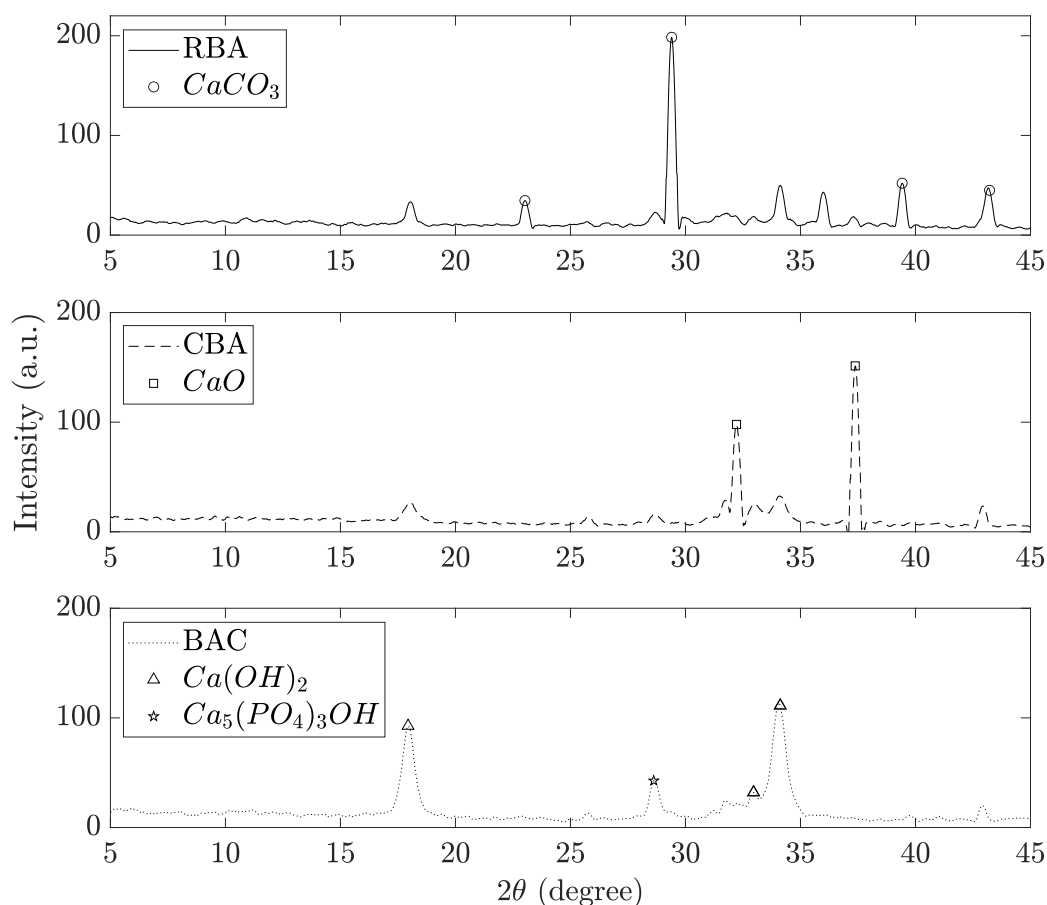


**Figure 3.** XRD spectra for raw bottom ash RBA, calcined bottom ash CBA, and catalyst (ash/ $\text{CaO}$  BAC) samples.

About catalytic properties of different calcium compounds, its oxide form ( $\text{CaO}$ ) has been reported to perform better than hydroxide ( $\text{Ca}(\text{OH})_2$ ) but with certain application problems, since  $\text{CaO}$  tends to absorb carbon dioxide from the environment, which deactivates the catalyst [43]. Moreover, carbonate ( $\text{CaCO}_3$ ) does not exhibit catalytic activity for biodiesel synthesis [43]. Finally, no performance comparisons with calcium phosphate have been reported.

## 2.2. Biodiesel Production

The industrial palm oil presents an acid value of  $2.35\text{ mg NaOH/g}$  while the waste frying oil (WFO) has  $0.38\text{ mg NaOH/g}$ . This property is relevant because a high acid value

added to the use of basic catalysts produces saponification, decreasing the performance of the catalyst.

Reducing the acid number of the residual palm oil is an option to improve the efficiency of the process. This can be achieved by neutralization with alkaline salts and subsequent separation [44] or by mixing oils with different levels of acidity. The latter has been successfully applied to produce biodiesel even from industrial waste, by mixing it with sunflower oil [45].

Mixing residual palm oil with WFO, in a 50:50 ratio, the total acid number of the mixture decreases to 1.30 mg NaOH/g, with this an adequate value to work with basic catalysts. The fatty acid profile of the mixture shows a high presence of saturated (palmitic acid 25.3%), monounsaturated (oleic acid 37.1%), and polyunsaturated (linoleic acid 30.2%) components.

The fatty acid profile has a direct relationship to cloud point (CP), cold filter plugging point (CFPP), and other cold flow properties. Palm oil biodiesel is composed of up to 38.8 wt% methyl palmitate and has relatively high CP = 16 °C and CFPP = 12 °C [46]. In comparison, biodiesel from oils with a higher proportion of unsaturated fatty acids, such as rapeseed oil-based biodiesel, has lower values: CP = −3 °C and CFPP = −9 °C [47]. Therefore, blending industrial palm oil with WFO not only helps to reduce the acid number and improve the transesterification process, but would also improve the cold flow properties of the biodiesel obtained, due to the higher proportion of unsaturated fatty acid methyl esters in its composition.

### 2.2.1. Experimental Design

To obtain biodiesel, ash impregnated with 10% calcium oxide was used as a basic catalyst. According to the proposed experimental design (Table 2), 15 experiments were carried out, with a random order of execution. The regression Equation (1) was generated from the experimental response using the full quadratic response surface model. A Box–Cox transformation using  $\lambda = 1.50$  was applied to the response data to normalize it and provide a more robust model, but it does not affect the goodness-of-fit of the regression model. The significance of the model was assessed by ANOVA test (Table 3). The experimental design together with the results of the regression model are presented in Table 2.

**Table 2.** Biodiesel yields from transesterification reactions from the experimental design and regression model using catalyst (BAC).

N° Run	N° Experiment	MR	CW	RT	% FAME	% FAME Model
1	8	14	6	4	42.13	43.39
2	15	10	6	3	89.00	88.22
3	6	14	6	2	74.66	78.09
4	5	6	6	2	68.30	67.50
5	2	14	4	3	69.57	64.95
6	10	10	8	2	95.61	92.89
7	12	10	8	4	73.69	73.04
8	7	6	6	4	65.10	60.92
9	3	6	8	3	70.77	75.02
10	1	6	4	3	64.00	64.10
11	14	10	6	3	89.12	88.22
12	11	10	4	4	65.74	69.52
13	9	10	4	2	80.67	81.24
14	4	14	8	3	72.43	72.33
15	13	10	6	3	86.40	88.22

On the ANOVA results, for the complete model,  $F$ -value = 13.10 and  $p$ -value = 0.006 were obtained, which means that there are differences between the means of the measurements for each experiment, and these differences are significant. Also within the model,



CW (catalyst concentration), RT,  $RT^2$  (reaction time),  $MR^2$  (alcohol ratio), and  $MR \times CW$  (two-factor interactions) are significant variables. Finally, the fitted  $R^2$  value ( $R^2 = 95.93\%$ ,  $R^2$  adjust. =  $88.61\%$ ) of the model indicates that the experimental data are close to the fitted regression line. Therefore: The regression model is able to largely interpret the variability of the experimental response (% FAME), the effect of the experimental variables on the response is significant, and finally, the prediction of the model on the response variable is significant.

**Table 3.** ANOVA regression model.

	GL	SC Adjst.	F-Value	p-Value
Model	9	48.115917	13.10	0.006
Linear	3	16.054225	13.11	0.008
MR	1	0.041089	0.10	0.764
CW	1	3.203072	7.85	0.038
RT	1	12.810064	31.38	0.003
Quadratic	3	28.573184	23.33	0.002
$MR^2$	1	25.663634	62.88	0.001
$CW^2$	1	0.450301	1.10	0.342
$RT^2$	1	4.337852	10.63	0.022
2-factor interactions	3	3.488507	2.85	0.144
$MR \times CW$	1	0.064078	0.16	0.708
$MR \times RT$	1	2.841467	6.96	0.046
$CW \times RT$	1	0.582963	1.43	0.286
Error	5	2.040844		
Lack of fit	3	1.888895	8.29	0.110
Pure error	2	0.15195		
Total	14	50.156761		

From the experimental design and the regression model, it was obtained that the best performance point (92.89% FAME) for the proposed catalyst is under the operating conditions: CW = 8%; MR = 10.36:1 and RT = 2.28 h. This coincides with what was observed in practice, where the best performance (95.61% FAME) was obtained for the conditions CW = 8%; MR= 10:1 and RT= 2 h.

Increasing the amount of catalyst significantly improves the FAME concentration (Figure 4—CW) due to the increased presence of basic sites (active species such as  $Ca(OH)_2$ ) available for the process. However, increasing the amount of catalyst by more than 8% may no longer have such a marked effect, as it could only increase the reaction rate, but not the conversion (FAME) of the reaction, since the latter is more related to the catalyst composition and not to the availability of the catalyst [27].

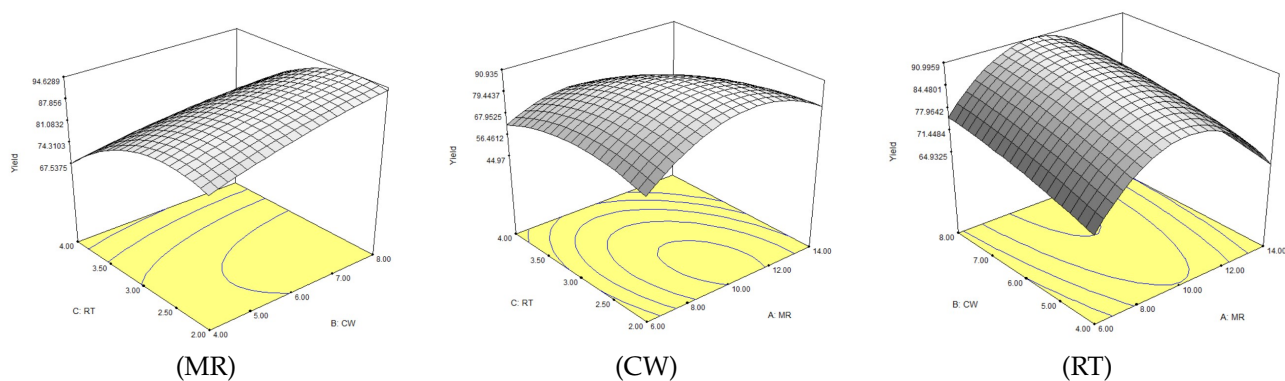


**Figure 4.** Contourplots for the factors molar ratio (MR), catalyst concentration (CW), and reaction time (RT). The response is optimal for low reaction times and for medium values for the others.

Using heterogeneous catalysts, an excess of alcohol is used to shift the equilibrium of the reaction towards the formation of FAME, which improves the performance of heterogeneous catalysts; however, it is not recommended to use ratios higher than 15:1 [37] since a higher concentration of methanol leads to a decrease in performance due to the increase in methanol-glycerol solubility that interferes in the separation of glycerol. The presence of the polar hydroxyl group in methanol favors the emulsification of the biodiesel, decreasing its purity [48].

The conversion of FAME did not improve with increasing reaction time (Figure 4—RT). In other heterogeneous catalysts, this behavior has been associated with the deactivation of active sites in the catalyst [49].

$$\text{FAME}^2 = -30222 + 4005 \text{ MR} + 2095 \text{ CW} + 8490 \text{ RT} - 164.8 \text{ MR}^2 - 87.3 \text{ CW}^2 - 1084 \text{ RT}^2 - 15.8 \text{ MR} \times \text{CW} - 210.7 \text{ MR} \times \text{RT} - 191 \text{ CW} \times \text{RT} \quad (1)$$

### 2.2.2. Catalyst Reuse

Reusability is a relevant feature in a heterogeneous catalyst to be used commercially. Reusability was studied by performing three successive reaction cycles with the optimum point parameters given by the experimental design and the recovery methods described in the methodology section. The main problem presented is that the mass of catalyst recovered by sedimentation was always lower with respect to the previous cycle, so the amount of reactants had to be adjusted to maintain the ratio between all the experiments. The yield in the conversion to FAME after three reaction cycles was 84% for the untreated catalyst, 99.4% for the calcination method at 900 °C, and 96.95% for the hexane washing method, so both recovery methods are equally effective in allowing the reuse of the catalyst. Regarding the behavior between cycles (Figure 5), when using the catalyst without a recovery method, there is always a downward trend in the yield [19,27]. As such, the proposed methods allow a more stable performance and perhaps extend the use of the catalyst for more cycles.

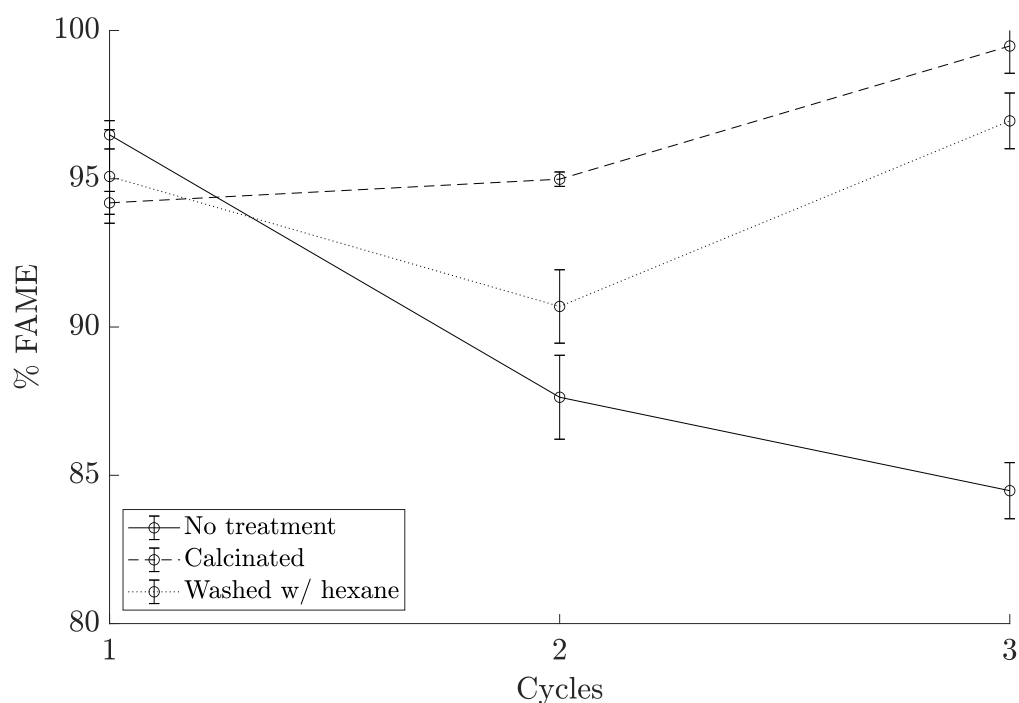


**Figure 5.** Yield of FAME according to number of cycles of use for different catalyst recovery methods.

FTIR analysis (Figure 6) was used to study the composition of the recovered catalysts to evaluate their stability and possible causes of deactivation. In the case of the basic oxides used to carry on the transesterification reaction, the leaching of metal ions into the



solution is a direct cause of catalyst deactivation. This is observed in the decrease of the peak associated with calcium hydroxide, since in the reused catalysts, it is much lower compared to the unused catalyst (BAC sample in Figure 2). However, using high amounts of catalyst at the beginning of the reaction usually overcomes this obstacle [28]. Another cause of deactivation could be the blockage of the catalytic active sites by intermediate species produced during the reaction, such as glycerol or unconverted oil [50]. Signal peaks are observed at  $2920\text{ cm}^{-1}$  and  $2850\text{ cm}^{-1}$ , which correspond to the vibration of  $\text{CH}_2$  groups, coinciding with those present in saturated fatty acids [51], so they must be unreacted oil residues. Another peak of interest appears at  $1740\text{ cm}^{-1}$ , attributed to axial deformation of the  $\text{C}=\text{O}$  double bond of the ester [52,53]. It is observed from the analysis that the calcination method effectively removes the unreacted fatty acid residues from the catalyst, but decreases the presence of  $\text{CaOH}_2$ , while the hexane wash is less effective in removing the residues, but retains the functional groups of  $\text{CaOH}_2$ .

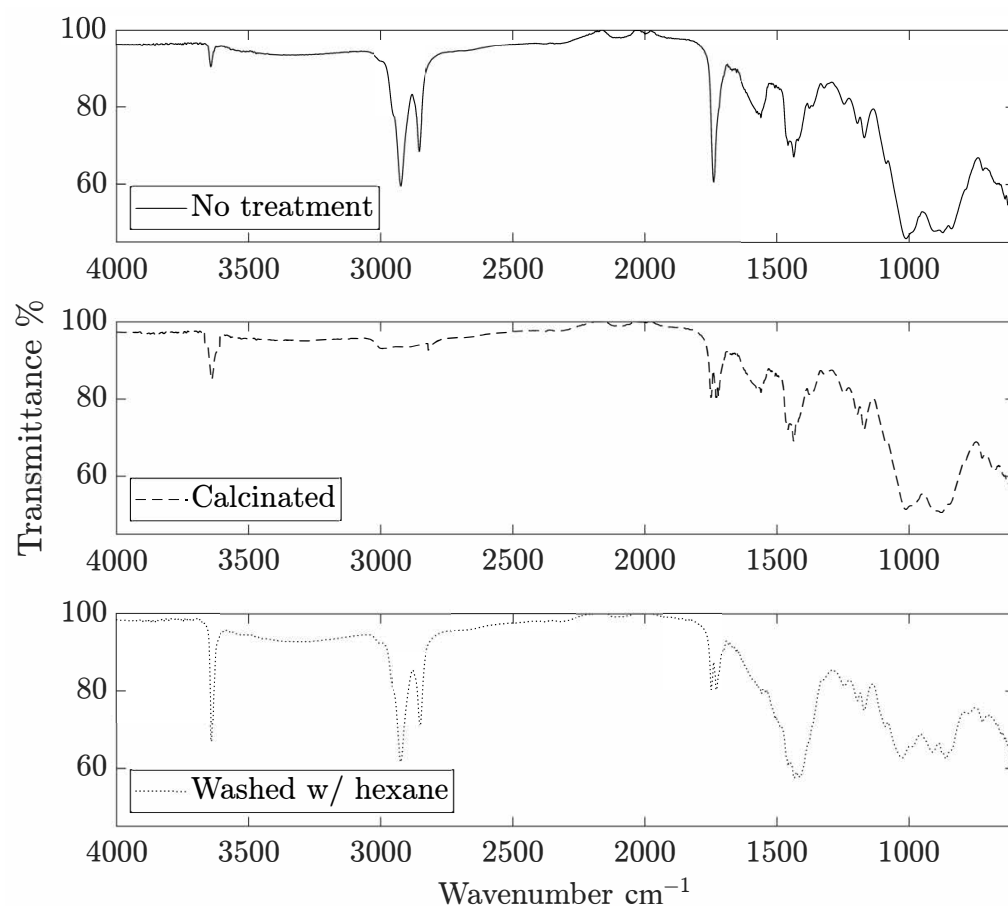


**Figure 6.** FTIR spectrum for catalyst samples after 3 cycles of use. Signal peaks associated with  $\text{CH}_2$  groups derived from oil residues are observed.

### 2.3. Biodiesel Properties

The key physicochemical properties of biodiesel are compared with the applicable EN 14214 Std. (Table 4). One of the most important properties is the concentration of esters (% FAME) in the biodiesel. The hexane washing method was the only one that provided a yield above the regulatory limit (96.5%) after three cycles of use; therefore, the rest of the properties are presented with respect to this sample. It is important that the properties comply with the established requirements, as they influence the performance of biodiesel in combustion engines, e.g., high density values have been associated with the presence of glycerol in the product, so a density below the  $900\text{ kg/m}^3$  limit indicates that the biodiesel will have no residues or by-products in its composition. On the other hand, to avoid coking in the injectors, the kinematic viscosity is a critical factor; in this case, the value is below

the upper limit of 5.0 mm<sup>2</sup>/s. The acid value is the only property among those studied that did not meet the regulatory limit, which may be due to the washing method. Although using a phosphoric acid solution is effective in removing calcium residues in the biodiesel, it can leave dissolved PO<sub>4</sub><sup>3−</sup> ions, increasing the final acidity of the product. To correct the acid value, a washing cycle with distilled water could be performed after washing with the acid solution.

**Table 4.** Properties of biodiesel compared to EN 14214 Std., optimal reaction conditions, and the third reuse cycle with the hexane washing step.

Properties	Washed w/Hexane (Third Cycle)	EN 14214 Std.
Kinematic viscosity at 40 °C (mm <sup>2</sup> /s)	4.87	Max. 5.00
Density at 15 °C (kg/m <sup>3</sup> )	862.0	Max. 900
Water content (mg/kg)	0.25	Max. 5.00
Biodiesel yield (wt%)	96.95	Min. 96.50
Acid value (mg KOH/g)	1.27	Max. 0.50

### 3. Materials and Methods

#### 3.1. Materials

Two types of waste frying oil were used: palm oil collected from a sausage manufacturer in the city of Temuco, Chile; and domestic waste oil (WFO). Density, acid value, and fatty acid profile of the collected oils were measured. For the catalyst, bottom ash collected from the burner of a biomass boiler fed with leftover material from forestry and food industry processes, collected during June 2022, was used; on the other hand, eggshells used to obtain CaO were separated from municipal solid waste (MSW). The reagents used were all of analytical grade (Scharlau, Spain).

#### 3.2. Catalyst Preparation

The method is similar to that reported by Abdul et al. [23], Chen et al. [12], and Chakraborty et al. [24] for other types of ash impregnated with eggshells. The bottom ash was calcined at 900 ± 5 °C for 2 h in a muffle furnace to remove unburned carbon residues that could interfere with the catalyst. Then to prepare a catalyst loaded with CaO at 10 wt%, 3 g of the resulting powder from the eggshell calcination was slowly added to 150 mL of distilled water to prepare an aqueous solution of Ca(OH)<sub>2</sub>. To this solution, 27 g of ash was subsequently added and mixed with constant magnetic stirring (500 rpm) for 4 h at 70 ± 1 °C. The solution was kept at rest for 24 h for the formation of Ca(OH)<sub>2</sub> precipitate on the ash support. The excess water was removed in a dry oven at 105 °C for 24 h. The powder was then calcined in a muffle furnace at 900 ± 5 °C for 2 h to obtain the ash-supported catalyst.

#### 3.3. Catalyst Characterization

The BET specific surface area, BJH pore volume, and pore size distribution were analyzed using a NOVA 1000e porosimeter (QUANTACHROME, Boynton Beach, FL, USA). This involved adsorbing and desorbing nitrogen at a temperature of 77 K on samples that were first dried and outgassed at 160 °C for a period of 16 h.

The particle size distribution of the samples was measured using a SALD-3101 (Shimadzu, Kyoto, Japan) laser diffraction particle size analyzer.

Scanning electron microscopy (SEM) and energy dispersive spectroscopy (EDS) were applied with a variable-pressure scanning electron microscope SU 3500 (Hitachi, Tokyo, Japan) to compare the microstructure of the catalysts produced and to analyze the chemical composition on the surface of each sample under operating conditions of 10 kV and 40 Pa.

Fourier transform infrared (FTIR) spectroscopy was conducted to characterize the surface functional groups using an Agilent Cary 630 FTIR (Agilent, Santa Clara, CA, USA) diamond ATR in the range of 600–4000 cm<sup>−1</sup>.

The crystalline phase of the samples was analyzed using a SmartLab powder X-ray diffractometer (Rigaku, Tokyo, Japan) coupled with Cu K $\alpha$  radiation.

### 3.4. Biodiesel Production

The method to obtain methyl esters (FAME) is known as transesterification [54]. A 50:50 mixture of waste frying oil and waste palm oil was used as a base for the transesterification process. A total of 50 g of oil blend was massified then added to a round flask and heated to 60 °C using a hotplate. A mixture of methanol and catalyst was added to the flask with the oil, then the researchers waited for the whole mixture to reach 60 °C. The amount of methanol and catalyst needed are given according to the experimental design. A condensation column was connected to the flask mouth to avoid methanol losses, then it was allowed to react during the time defined according to the experimental design. After the reaction time elapsed, the sample was allowed to cool and transferred to a decanting funnel. After 20 h of sedimentation, 3 phases were differentiated; the upper phase (biodiesel) was extracted from the decanting funnel and using a rotoevaporator at 60 °C, and the residual methanol was separated from the biodiesel until a constant volume was obtained. The biodiesel was then poured back into the funnel and washed by adding a solution of water and phosphoric acid at 3% vol/vol, at 60 °C. The slight acidity in the washing solution together with its higher temperature improves the ability to remove catalyst residues and reaction residues. The process was repeated until there were no more visible solid residues in the biodiesel.

#### 3.4.1. Experimental Design

A Box–Behnken response surface design was applied. The independent variables and their levels were as follows: alcohol molar ratio (MR) (1:6, 1:10, and 1:14 mol<sub>oil</sub>:mol<sub>alcohol</sub>), catalyst concentration (CW) (4, 6, and 8 % wt<sub>oil</sub>), and reaction time (RT) (2, 3, and 4 h). The dependent variable of the process is the concentration of FAME in the obtained biodiesel. Box–Behnken designs typically have fewer design points and are less expensive to perform than central composite designs with the same number of factors [55]. Statistical analysis was performed with the Design-Expert 6.0 (trial version) software.

#### 3.4.2. Catalyst Reusability

To evaluate the reuse of the catalyst, the transesterification reaction was carried out at the optimum reaction conditions obtained from the experimental design, and three different methods of catalyst recovery were tested. In the first case, the catalyst was separated from the mixture by sedimentation, dried at 105 °C, and reused for the next reaction cycle. In the second case, it was separated by sedimentation, washed with hexane to clean the catalyst surface, dried at 105 °C, and reused for the next cycle. For the last case, the catalyst was separated in the same way and then it was calcined at 900 °C to be used in the next cycle. Three reaction cycles were performed for each recovery method, and the performance of each recovery method was compared according to the concentration of FAME in the biodiesel obtained.

#### 3.4.3. Biodiesel Properties

Density was determined using a densimeter floating vertically in the liquid (oil or FAME), according to EN-12185. The kinematic viscosity was determined as a function of the time it takes for a volume of liquid to flow by gravity at 40 °C through a calibrated capillary viscosimeter (CFR 100 type), according to ASTM D445-03 method. The acid value is defined as the number of mg of KOH or NaOH necessary to neutralize the free fatty acids of 1 g of oil or fat, obtained by means of an acid–base titration method adapted from the ISO 660 standard [56].

Adapted from EN-14103, the determination of the percentage of fatty acid methyl esters present in a sample and their concentration is obtained by gas chromatography using internal calibration. A Perkin Elmer Clarus 600 gas chromatograph (GC/MS) (PerkinElmer,

Waltham, MA, USA) equipped with Elite-5MS capillary column (PerkinElmer, Waltham, MA, USA) with a length of 30 m, a thickness of 0.1 µm and an internal diameter of 0.25 mm was used. Vials were prepared by adding 10 µL of sample to 233 µL of methyl heptadecanoate as the internal standard (initial concentration of 2060 mg/L). The yield of FAME was calculated using (Equation (2)):

$$\%FAME_{\text{yield}}(\%wt) = \frac{FAME(\%wt)}{TFA(\%wt)} \times 100 \quad (2)$$

where FAME represents the GC quantification of fatty acid methyl esters and TFA corresponds to the gravimetric quantification of transesterifiable lipids (88.98%). These compounds were determined by alkaline saponification and subsequent esterification to fatty acid methyl esters (FAME) according to the AOCS method (Ce 2-66) [57].

#### 4. Conclusions

In conclusion, biomass boiler bottom ash can be used as a heterogeneous catalyst for biodiesel production. This waste is characterized as a mesoporous material with high calcium content in the form of carbonate. Wet impregnation with eggshells improves its performance by increasing the presence of calcium and provides a greater availability of active sites since the aggregates of larger ash particles are broken. The subsequent calcination at 900 °C allows for transforming the calcium carbonate into calcium oxide and calcium hydroxide, which have higher catalytic capacity. The developed catalyst performs well under medium reaction conditions (CW = 8; MR = 1:10, and RT = 2), giving a 95% yield in FAME conversion according to the regression model obtained from the response surface experimental design. When studying the reusability of the catalyst, it was observed that after three cycles of use without treatment, it reached up to 84.48% in the conversion of FAME, while when using recovery methods such as calcination or washing with hexane, it was able to maintain the reaction yield (99.48% and 96.95%, respectively). The main causes of catalyst deactivation were the loss of active sites by leaching of calcium ions, contamination by unreacted oil, and the change of the active phase from calcium oxide to calcium carbonate. Finally, regarding the properties of the biodiesel obtained, it complied with the limits set by the EN 14214 standard [58] in terms of density, viscosity, water content, and FAME concentration. As for the acidity value, the biodiesel did not comply with the standard, which may be the result of using an acid solution in the washing of the biodiesel.

**Author Contributions:** Conceptualization, B.N. and M.E.G.; methodology, M.E.G.; software, B.N.; validation, B.N., M.E.G., and J.Ñ.; formal analysis, B.N. and M.E.G.; investigation, B.N. and M.E.G.; resources, M.E.G.; data curation, B.N. and J.Ñ.; writing—original draft preparation, B.N. and J.Ñ.; writing—review and editing, M.E.G., J.M.R.-G. and N.G. All authors have read and agreed to the published version of the manuscript.

**Funding:** This research received no external funding.

**Data Availability Statement:** The data presented in this study are available on request from the corresponding author. The data are not publicly available due to privacy.

**Acknowledgments:** Acknowledgments to the Centre for Waste Management and Bioenergy and to the Scientific and Technological Bioresources Nucleus—BIOREN.

**Conflicts of Interest:** The authors declare no conflicts of interest. The funders had no role in the design of the study; in the collection, analyses, or interpretation of data; in the writing of the manuscript; or in the decision to publish the results.

#### References

1. del Consuelo Ortiz Tapia, M.; Alamilla, P.G.; Gálvez, L.M.L.; Quezada, M.I.A.; Alamilla, R.G.; Chávez, M.A.L. Biodiesel production from crude palm oil (*Elaeis guineensis* Jacq). Ascending path method application. *Acta Univ.* **2016**, *26*, 3–10. [CrossRef]
2. Yan, Y. Biodiesel. In *Encyclopedia of Food Grains*, 2nd ed.; Elsevier: Amsterdam, The Netherlands, 2016; Volume 3, pp. 245–250. [CrossRef]

3. Vargas, E.M.; Neves, M.C.; Tarelho, L.A.; Nunes, M.I. Solid catalysts obtained from wastes for FAME production using mixtures of refined palm oil and waste cooking oils. *Renew. Energy* **2019**, *136*, 873–883. [\[CrossRef\]](#)
4. Demirbas, A. Biodiesel from waste cooking oil via base-catalytic and supercritical methanol transesterification. *Energy Convers. Manag.* **2009**, *50*, 923–927. [\[CrossRef\]](#)
5. Mumtaz, M.W.; Adnan, A.; Mukhtar, H.; Rashid, U.; Danish, M. Biodiesel Production Through Chemical and Biochemical Transesterification: Trends, Technicalities, and Future Perspectives. In *Clean Energy for Sustainable Development: Comparisons and Contrasts of New Approaches*; Academic Press: Cambridge, MA, USA, 2017; pp. 465–485. [\[CrossRef\]](#)
6. Baskar, G.; Kalavathy, G.; Aiswarya, R.; Selvakumari, I.A. Advances in bio-oil extraction from nonedible oil seeds and algal biomass. In *Advances in Eco-Fuels for a Sustainable Environment*; Woodhead Publishing: Sawston, UK, 2019; pp. 187–210. [\[CrossRef\]](#)
7. Abdullah, S.H.Y.S.; Hanapi, N.H.M.; Azid, A.; Umar, R.; Juahir, H.; Khatoon, H.; Endut, A. A review of biomass-derived heterogeneous catalyst for a sustainable biodiesel production. *Renew. Sustain. Energy Rev.* **2017**, *70*, 1040–1051. [\[CrossRef\]](#)
8. Takagaki, A.; Toda, M.; Okamura, M.; Kondo, J.N.; Hayashi, S.; Domen, K.; Hara, M. Esterification of higher fatty acids by a novel strong solid acid. *Catal. Today* **2006**, *116*, 157–161. [\[CrossRef\]](#)
9. Maroa, S.; Inambao, F. A review of sustainable biodiesel production using biomass derived heterogeneous catalysts. *Eng. Life Sci.* **2021**, *21*, 790–824. [\[CrossRef\]](#) [\[PubMed\]](#)
10. Mierczynski, P.; Ciesielski, R.; Kedziora, A.; Maniukiewicz, W.; Shtyka, O.; Kubicki, J.; Albinska, J.; Maniecki, T.P. Biodiesel Production on MgO, CaO, SrO and BaO Oxides Supported on (SrO)(Al<sub>2</sub>O<sub>3</sub>) Mixed Oxide. *Catal. Lett.* **2015**, *145*, 1196–1205. [\[CrossRef\]](#)
11. Sahu, O. Characterisation and utilization of heterogeneous catalyst from waste rice-straw for biodiesel conversion. *Fuel* **2021**, *287*, 119543. [\[CrossRef\]](#)
12. Chen, G.Y.; Shan, R.; Shi, J.F.; Yan, B.B. Transesterification of palm oil to biodiesel using rice husk ash-based catalysts. *Fuel Process. Technol.* **2015**, *133*, 8–13. [\[CrossRef\]](#)
13. Roschat, W.; Siritanon, T.; Yoosuk, B.; Promarak, V. Rice husk-derived sodium silicate as a highly efficient and low-cost basic heterogeneous catalyst for biodiesel production. *Energy Convers. Manag.* **2016**, *119*, 453–462. [\[CrossRef\]](#)
14. Obadih, A.; Swaroopa, G.A.; Kumar, S.V.; Jeganathan, K.R.; Ramasubbu, A. Biodiesel production from Palm oil using calcined waste animal bone as catalyst. *Bioresour. Technol.* **2012**, *116*, 512–516. [\[CrossRef\]](#)
15. Aleman-Ramirez, J.; Moreira, J.; Torres-Arellano, S.; Longoria, A.; Okoye, P.U.; Sebastian, P. Preparation of a heterogeneous catalyst from moringa leaves as a sustainable precursor for biodiesel production. *Fuel* **2021**, *284*, 118983. [\[CrossRef\]](#)
16. Thomas, M.; Jewell, R.; Jones, R. *Coal Fly Ash as a Pozzolan*; Elsevier: Amsterdam, The Netherlands, 2017; pp. 121–154. [\[CrossRef\]](#)
17. Cabrera, M.; Galvin, A.P.; Agrela, F.; Carvajal, M.D.; Ayuso, J. Characterisation and technical feasibility of using biomass bottom ash for civil infrastructures. *Constr. Build. Mater.* **2014**, *58*, 234–244. [\[CrossRef\]](#)
18. Elliott, A.; Mahmood, T.; Kamal, A. Boiler ash utilization in the Canadian pulp and paper industry. *J. Environ. Manag.* **2022**, *319*, 115728. [\[CrossRef\]](#) [\[PubMed\]](#)
19. Adepoju, T. Synthesis of biodiesel from *Annona muricata*—*Calophyllum inophyllum* oil blends using calcined waste wood ash as a heterogeneous base catalyst. *MethodsX* **2021**, *8*, 101188. [\[CrossRef\]](#)
20. Misra, M.K.; Ragland, K.W.; Baker, A.J. Wood ash composition as a function of furnace temperature. *Biomass Bioenergy* **1993**, *4*, 103–116. [\[CrossRef\]](#)
21. Chouhan, A.P.S.; Sarma, A.K. Biodiesel production from *Jatropha curcas* L. oil using *Lemna perpusilla* Torrey ash as heterogeneous catalyst. *Biomass Bioenergy* **2013**, *55*, 386–389. [\[CrossRef\]](#)
22. Deka, D.C.; Basumatary, S. High quality biodiesel from yellow oleander (*Thevetia peruviana*) seed oil. *Biomass Bioenergy* **2011**, *35*, 1797–1803. [\[CrossRef\]](#)
23. Mutalib, A.A.A.; Ibrahim, M.L.; Matmin, J.; Kassim, M.F.; Mastuli, M.S.; Taufiq-Yap, Y.H.; Shohaimi, N.A.M.; Islam, A.; Tan, Y.H.; Kaus, N.H.M. SiO<sub>2</sub>-Rich Sugar Cane Bagasse Ash Catalyst for Transesterification of Palm Oil. *BioEnergy Res.* **2020**, *13*, 986–997. [\[CrossRef\]](#)
24. Chakraborty, R.; Bepari, S.; Banerjee, A. Transesterification of soybean oil catalyzed by fly ash and egg shell derived solid catalysts. *Chem. Eng. J.* **2010**, *165*, 798–805. [\[CrossRef\]](#)
25. Ho, W.W.S.; Ng, H.K.; Gan, S. Development and characterisation of novel heterogeneous palm oil mill boiler ash-based catalysts for biodiesel production. *Bioresour. Technol.* **2012**, *125*, 158–164. [\[CrossRef\]](#) [\[PubMed\]](#)
26. Ho, W.W.S.; Ng, H.K.; Gan, S.; Tan, S.H. Evaluation of palm oil mill fly ash supported calcium oxide as a heterogeneous base catalyst in biodiesel synthesis from crude palm oil. *Energy Convers. Manag.* **2014**, *88*, 1167–1178. [\[CrossRef\]](#)
27. Maneerung, T.; Kawi, S.; Wang, C.H. Biomass gasification bottom ash as a source of CaO catalyst for biodiesel production via transesterification of palm oil. *Energy Convers. Manag.* **2015**, *92*, 234–243. [\[CrossRef\]](#)
28. Yoosuk, B.; Udomsap, P.; Puttasawat, B.; Krasae, P. Modification of calcite by hydration–dehydration method for heterogeneous biodiesel production process: The effects of water on properties and activity. *Chem. Eng. J.* **2010**, *162*, 135–141. [\[CrossRef\]](#)
29. Hoyos-Montilla, A.A.; Puertas, F.; Mosquera, J.M.; Tobón, J.I. Infrared spectra experimental analyses on alkali-activated fly ash-based binders. *Spectrochim. Acta Part A Mol. Biomol. Spectrosc.* **2022**, *269*, 120698. [\[CrossRef\]](#)
30. Ren, F.; Ding, Y.; Leng, Y. Infrared spectroscopic characterization of carbonated apatite: A combined experimental and computational study. *J. Biomed. Mater. Res. Part A* **2014**, *102*, 496–505. [\[CrossRef\]](#) [\[PubMed\]](#)
31. Haq, E.U.; Padmanabhan, S.K.; Licciulli, A. Synthesis and characteristics of fly ash and bottom ash based geopolymers—A comparative study. *Ceram. Int.* **2014**, *40*, 2965–2971. [\[CrossRef\]](#)



32. Fleet, M.E. Infrared spectra of carbonate apatites v2 Region bands. *Biomaterials* **2009**, *30*, 1473–1481. [\[CrossRef\]](#)
33. Cienkosz-Stepańczak, B.; Szostek, K.; Lisowska-Gaczorek, A. Optimizing FTIR method for characterizing diagenetic alteration of skeletal material. *J. Archaeol. Sci. Rep.* **2021**, *38*, 103059. [\[CrossRef\]](#)
34. Yin.; Yin.; Wu.; Qi.; Tian.; Zhang.; Hu.; Feng. Characterization of Coals and Coal Ashes with High Si Content Using Combined Second-Derivative Infrared Spectroscopy and Raman Spectroscopy. *Crystals* **2019**, *9*, 513. [\[CrossRef\]](#)
35. Naemchan, K.; Meejoo, S.; Onreabroy, W.; Limsuwan, P. Temperature Effect on Chicken Egg Shell Investigated by XRD, TGA and FTIR. *Adv. Mater. Res.* **2008**, *55–57*, 333–336. [\[CrossRef\]](#)
36. de Oliveira Romano, R.C.; Bernardo, H.M.; Maciel, M.H.; Pileggi, R.G.; Cincotto, M.A. Using isothermal calorimetry, X-ray diffraction, thermogravimetry and FTIR to monitor the hydration reaction of Portland cements associated with red mud as a supplementary material. *J. Therm. Anal. Calorim.* **2019**, *137*, 1877–1890. [\[CrossRef\]](#)
37. Uprety, B.K.; Chaiwong, W.; Ewelike, C.; Rakshit, S.K. Biodiesel production using heterogeneous catalysts including wood ash and the importance of enhancing byproduct glycerol purity. *Energy Convers. Manag.* **2016**, *115*, 191–199. [\[CrossRef\]](#)
38. Gualtieri, M.L.; Romagnoli, M.; Miselli, P.; Cannio, M.; Gualtieri, A.F. Full quantitative phase analysis of hydrated lime using the Rietveld method. *Cem. Concr. Res.* **2012**, *42*, 1273–1279. [\[CrossRef\]](#)
39. Kumar, K.V.; Subha, T.J.; Ahila, K.; Ravindran, B.; Chang, S.; Mahmoud, A.H.; Mohammed, O.B.; Rath, M. Spectral characterization of hydroxyapatite extracted from Black Sumatra and Fighting cock bone samples: A comparative analysis. *Saudi J. Biol. Sci.* **2021**, *28*, 840–846. [\[CrossRef\]](#)
40. Suchanek, K.; Bartkowiak, A.; Perzanowski, M.; Marszałek, M. From monetite plate to hydroxyapatite nanofibers by monoethanolamine assisted hydrothermal approach. *Sci. Rep.* **2018**, *8*, 15408. [\[CrossRef\]](#)
41. Sharma, M.; Khan, A.A.; Puri, S.; Tuli, D. Wood ash as a potential heterogeneous catalyst for biodiesel synthesis. *Biomass Bioenergy* **2012**, *41*, 94–106. [\[CrossRef\]](#)
42. Pavlović, S.M.; Marinković, D.M.; Kostić, M.D.; Janković-Častvan, I.M.; Mojović, L.V.; Stanković, M.V.; Veljković, V.B. A CaO/zeolite-based catalyst obtained from waste chicken eggshell and coal fly ash for biodiesel production. *Fuel* **2020**, *267*, 117171. [\[CrossRef\]](#)
43. Kouzu, M.; Kasuno, T.; Tajika, M.; Sugimoto, Y.; Yamanaka, S.; Hidaka, J. Calcium oxide as a solid base catalyst for transesterification of soybean oil and its application to biodiesel production. *Fuel* **2008**, *87*, 2798–2806. [\[CrossRef\]](#)
44. Cvengroš, J.; Cvengrošová, Z. Used frying oils and fats and their utilization in the production of methyl esters of higher fatty acids. *Biomass Bioenergy* **2004**, *27*, 173–181. [\[CrossRef\]](#)
45. Usta, N.; Ozturk, E.; Can, O.; Conkur, E.; Nas, S.; Çon, A.; Can, A.; Topcu, M. Combustion of biodiesel fuel produced from hazelnut soapstock/waste sunflower oil mixture in a Diesel engine. *Energy Convers. Manag.* **2005**, *46*, 741–755. [\[CrossRef\]](#)
46. Benjumea, P.; Agudelo, J.; Agudelo, A. Basic properties of palm oil biodiesel–diesel blends. *Fuel* **2008**, *87*, 2069–2075. [\[CrossRef\]](#)
47. Rashid, U.; Anwar, F. Production of biodiesel through optimized alkaline-catalyzed transesterification of rapeseed oil. *Fuel* **2008**, *87*, 265–273. [\[CrossRef\]](#)
48. Viriya-empikul, N.; Krasae, P.; Nualpaeng, W.; Yoosuk, B.; Faungnawakij, K. Biodiesel production over Ca-based solid catalysts derived from industrial wastes. *Fuel* **2012**, *92*, 239–244. [\[CrossRef\]](#)
49. Jitjamnong, J.; Thunyaratchatanon, C.; Luengnaruemitchai, A.; Kongrit, N.; Kasetsomboon, N.; Sopajarn, A.; Chuaykarn, N.; Khantikulanan, N. Response surface optimization of biodiesel synthesis over a novel biochar-based heterogeneous catalyst from cultivated (*Musa sapientum*) banana peels. *Biomass Convers. Biorefinery* **2021**, *11*, 2795–2811. [\[CrossRef\]](#)
50. Volli, V.; Purkait, M.K.; Shu, C.M. Preparation and characterization of animal bone powder impregnated fly ash catalyst for transesterification. *Sci. Total Environ.* **2019**, *669*, 314–321. [\[CrossRef\]](#)
51. Mukhametov, A.; Mamayeva, L.; Kazhymurat, A.; Akhlan, T.; Yerbulekova, M. Study of vegetable oils and their blends using infrared reflectance spectroscopy and refractometry. *Food Chem. X* **2023**, *17*, 100386. [\[CrossRef\]](#) [\[PubMed\]](#)
52. González, M.; Cea, M.; Reyes, D.; Romero-Hermoso, L.; Hidalgo, P.; Meier, S.; Benito, N.; Navia, R. Functionalization of biochar derived from lignocellulosic biomass using microwave technology for catalytic application in biodiesel production. *Energy Convers. Manag.* **2017**, *137*, 165–173. [\[CrossRef\]](#)
53. Silva, G.A.M.; Rós, P.C.M.D.; Souza, L.T.A.; Costa, A.P.O.; de Castro, H.F. Physico-chemical, spectroscopical and thermal characterization of biodiesel obtained by enzymatic route as a tool to select the most efficient immobilized lipase. *Braz. J. Chem. Eng.* **2012**, *29*, 39–47. [\[CrossRef\]](#)
54. Gerpen, J.V.; Knothe, G.; Haas, M.J.; Schultz, A.K.; Banavali, R.; Topp, K.D.; Vandersall, M.T. Biodiesel Production. In *The Biodiesel Handbook*, 2nd ed.; AOCS Press: Urbana, IL, USA, 2010; pp. 31–96. [\[CrossRef\]](#)
55. Dharma, S.; Masjuki, H.; Ong, H.C.; Sebayang, A.; Silitonga, A.; Kusumo, F.; Mahlia, T. Optimization of biodiesel production process for mixed *Jatropha curcas*–*Ceiba pentandra* biodiesel using response surface methodology. *Energy Convers. Manag.* **2016**, *115*, 178–190. [\[CrossRef\]](#)
56. ISO 660; Animal and Vegetable Fats and Oils—Determination of Acid Value and Acidity. International Organization for Standardization: Geneva, Switzerland, 2020.
57. AOCS. *AOCS Methods for Biodiesel Feedstock Quality*, 6th ed.; AOCS Press: Urbana, IL, USA, 2012.
58. EN14214; Liquid Petroleum Products. Fatty Acid Methyl Esters (FAME) for Use in Diesel Engines and Heating Applications. Requirements and Test Methods. European Standard: Brussel, Belgium, 2021.



---

**Disclaimer/Publisher's Note:** The statements, opinions and data contained in all publications are solely those of the individual author(s) and contributor(s) and not of MDPI and/or the editor(s). MDPI and/or the editor(s) disclaim responsibility for any injury to people or property resulting from any ideas, methods, instructions or products referred to in the content.